IET Generation, Transmission & Distribution

*Special Issue: Optimal Utilisation of Storage Systems in Transmission and Distribution Systems*

# Determination of the optimal installation site and capacity of battery energy storage system in distribution network integrated with distributed generation

ISSN 1751-8687
Received on 30th January 2015
Revised on 9th October 2015
Accepted on 10th October 2015
doi: 10.1049/iet-gtd.2015.0130
www.ietdl.org

*Jun Xiao*[1] ✉, *Zequn Zhang*[1], *Linquan Bai*[2], *Haishen Liang*[1]

[1]*Key Laboratory of Smart Grid of Ministry of Education, Tianjin University, Tianjin 300072, People's Republic of China*
[2]*Department of Electrical Engineering and Computer Science, University of Tennessee, Knoxville, TN 37996, USA*
✉ *E-mail: xiaojun@tju.edu.cn*

**Abstract:** The presence of distributed generation (DG), represented by photovoltaic generation and wind generation, brings new challenges to distribution network operation. To accommodate the integration of DG, this study proposes a bi-level optimisation model to determine the optimal installation site and the optimal capacity of battery energy storage system (BESS) in distribution network. The outer optimisation determines the optimal site and capacity of BESS aiming at minimising total net present value (NPV) of the distribution network within the project life cycle. Then optimal power flow (OPF) and BESS capacity adjustment are implemented in the inner optimisation. OPF optimises the scheduling of BESS and network losses. On the basis of optimal scheduling of BESS, a novel capacity adjustment method is further proposed to achieve the optimal BESS capacity considering battery lifetime for minimising the NPV of BESS. Finally, the proposed method is performed on a modified IEEE 33-bus system and proven to be more effective comparing with an existing method without BESS capacity adjustment.

## 1 Introduction

In recent years, increasing distributed generation (DG), such as wind turbine (WT) and photovoltaic (PV), is integrated in distribution network (DN). There are several benefits that DG offers, such as loss reduction, voltage profile improvement, and reliability enhancement. However, the randomness and variability of DG bring negative impact on the operation of DN. Battery energy storage system (BESS) is regarded as one of the key solutions to accommodate the integration of DG. Due to the high cost of BESS, the problem of BESS allocation has recently received a lot of attention from power system researchers. Extensive work has been carried out on the capacity optimisation of a single BESS [1–4]. BESS is installed at the node connecting DG to the grid, or integrated on the DG side. Most of them focus on the capacity optimisation of a single BESS without considering the placement of BESS. However, in DN, the network losses and voltage drop are important issues such that the location of BESS has a significance impact on system operation. It is necessary to optimise both the installation site and capacity of BESS in DN such that multiple BESSs can work coordinately to reduce network losses and minimise the total cost.

In existing literature, there are a few works that address optimal sizing and siting of BESS in DN. In [5], optimal sizing and siting decisions for BESS in DN are obtained through a cost–benefit analysis method, with the goal of the optimisation to maximise the DN operator profits from energy transactions, investment and operation cost savings. The locations of BESS are optimised based on energy loss sensitivity, and then BESS capacities are determined through particle swarm optimisation in [6]. Nick *et al.* [7] adapt a second-order cone programming approach to formulate the problem of the optimal allocation of dispersed storage systems in active DNs. In the planning model, the lifetime of BESS is assumed to be 5 years. In [8], an analytical method for optimal siting and sizing of distributed energy storage systems (DESSs) at the peak hours is proposed to achieve energy loss reduction and maximise the profits from energy arbitrage. However, the investment cost of DESSs is not considered. In [9], the authors adopt genetic algorithm (GA) to optimise allocation of DESSs aiming at minimising network losses and deferring network upgrading. Further, in [10], they improved this model to include the impact of charging/discharging efficiency and state of charge (SOC) limits. To minimise the overall investment and network losses, a combination of GA with dynamic programming is presented in [11] to optimally determine the siting and capacity of DESSs. In [12], the BESS is considered either as a controllable load or controllable generator. The site and capacity of BESS are optimised by GA with the objective of maximising wind power utilisation, and the charging/discharging power of BESS is optimised by probabilistic optimal power flow. It comes to our attention that in above relevant works for multiple BESS planning in DN, the impact of charging/discharging cycles and depth of discharge (DOD) levels on the battery lifetime is not modelled in detail. The battery lifetime is usually assumed to be a fixed number of charging/discharging cycles regardless of DOD variations or just a predefined constant number.

In this paper, a bi-level optimisation model is proposed to optimally determine the siting and sizing of multiple BESSs in DN aiming at minimising the total net present value (NPV) of the DN within the project life cycle. The outer optimisation determines the optimal sites and capacity of BESSs to minimise the total NPV of the DN. Optimal power flow (OPF) and BESS capacity adjustment are implemented in the inner optimisation. OPF optimises the scheduling of BESS and network losses. On the basis of optimal scheduling of BESS, the BESS capacity adjustment is further proposed to achieve the optimal capacity of BESS considering battery lifetime. The BESS model is presented in detail considering the round-trip efficiency and SOC limits. In addition, the lifetime prediction model of BESS is built and rain-flow counting algorithm is adapted to evaluate the lifetime of BESS subjected to charging/discharging cycles and DOD. The BESS lifetime model is incorporated into the battery capacity adjustment of the inner optimisation. Finally, the effectiveness of the proposed method is verified on a modified IEEE 33-bus system.

## 2 Optimisation model for siting and sizing of BESS in DN

An optimisation model is built to determine the optimal site and capacity of BESS in DN. In finance, NPV is defined as the sum of the present values of incoming and outgoing cash flows over a period of time. An important feature of NPV is that it encompasses the concept of time value of money. NPV takes into consideration that money spent or obtained in future periods will have a different value with money spent or obtained in the present [13]. A major drawback of NPV is that it assumes the discount rate to be constant during the planning horizon, which might bring some errors. However, for a long-term planning, such a small error is acceptable. NPV is widely used for investment decision making in planning problems over a long project life cycle. For instance, in [14], the authors presented a NPV-based economic evaluation methodology to assess the impact of energy storage costs on economic performance in a distribution substation. In [15], NPV is adopted as an economy criterion in a methodology for the optimal allocation and economic analysis of energy storage system in microgrids. In [16], transmission power system structure is optimised by finding the optimal power line type with the objective of minimising NPV of the total cost including investment cost and operating costs. Therefore, NPV is also adopted as the objective in this work to determine the optimal installation site and capacity of BESS from an economic perspective. In the optimisation model, the objective is to minimise the NPV of DN during the project life cycle. The constraints include power flow balance, branch flow limits, BESS efficiency, and charging/discharging characteristics. The optimisation model is formulated as follows

$$f = \min\{\mathrm{NPV}\} \tag{1}$$

$$P_{\mathrm{E\_BESS}} = N \times P_{\mathrm{E\_unit}} \tag{2}$$

$$E_{\mathrm{E\_BESS}} = N \times E_{\mathrm{E\_unit}} \tag{3}$$

$$P_{\mathrm{DG}} + P_{\mathrm{HG}} + P_{\mathrm{BESS}} + P_{\mathrm{LOSS}} = P_{\mathrm{L}} \tag{4}$$

$$Q_{\mathrm{DG}} + Q_{\mathrm{HG}} + Q_{\mathrm{BESS}} + Q_{\mathrm{LOSS}} = Q_{\mathrm{L}} \tag{5}$$

$$\eta_{\mathrm{d}} = \eta_{\mathrm{c}} = \sqrt{\eta} \tag{6}$$

$$S_{ij\,\min} \le S_{ij} \le S_{ij\,\max} \tag{7}$$

$$1 \le N_{\mathrm{BESS}} \le N_{\mathrm{node}} \tag{8}$$

$$V_{\min} \le V_{jr} \le V_{\max}, \quad j = 0, 1, \ldots, N_{\mathrm{node}} \tag{9}$$

$$\mathrm{SOC}_{\min} \le \mathrm{SOC}_{\mathrm{r}}(i) \le \mathrm{SOC}_{\max}, \quad i = 0, 1, \ldots, N_{\mathrm{s}} \tag{10}$$

where $P_{\mathrm{E\_BESS}}$ and $E_{\mathrm{E\_BESS}}$ are the total power capacity and energy capacity of BESS, respectively; $P_{\mathrm{E\_unit}}$ and $E_{\mathrm{E\_unit}}$ are the power capacity and energy capacity of a single battery, respectively; and $N$ is the total number of batteries in the BESS.

Equations (4) and (5) represent the power flow balance constraint. $P_{\mathrm{DG}}$, $P_{\mathrm{HG}}$, $P_{\mathrm{BESS}}$, $P_{\mathrm{LOSS}}$, and $P_{\mathrm{L}}$ are the active power of DG, the main grid, BESS, line loss, and load, respectively. $Q_{\mathrm{DG}}$, $Q_{\mathrm{HG}}$, $Q_{\mathrm{BESS}}$, $Q_{\mathrm{LOSS}}$, and $Q_{\mathrm{L}}$ are the reactive power of DG, the main grid, BESS, line loss, and load, respectively.

BESS efficiency is considered in (6). $\eta_{\mathrm{d}}$ and $\eta_{\mathrm{c}}$ are the efficiencies of discharge, charge and $\eta$ is the overall round-trip efficiency.

The branch flow limit is shown in (7). $S_{ij\max}$ and $S_{ij\min}$ are the upper and lower power limits of line $ij$, and $S_{ij}$ is the apparent power on line $ij$.

Installation site node constraint is presented in (8), $N_{\mathrm{BESS}}$ is the number of BESSs, and $N_{\mathrm{node}}$ is the number of nodes that are available for BESS integration in DN.

Voltage constraints are considered in (9). $V_{\max}$ and $V_{\min}$ are the upper and lower limits of the node voltages and $V_{jr}$ is the voltage at node $j$.

To avoid the impact of over charge/discharge on battery lifetime, SOC constraints of BESS are considered in (10). $\mathrm{SOC}_{\min}$ and $\mathrm{SOC}_{\max}$ are the SOC operating bounds, and $N_{\mathrm{s}}$ is the number of sample data.

The power fluctuation characteristic of DG and load is addressed in the model. Typical daily data is commonly used to represent whole year.

## 3 Solution algorithm

### 3.1 Method flowchart

GA is applicable to solve constrained non-linear problems. GA is implemented in this work to solve the optimisation model. A bi-level optimisation solution algorithm is designed to solve the proposed model in Section 2. Steps involved in the algorithm are shown in the flowchart in Fig. 1.

*Step 1:* Input data of load, DG power, network topology of DN, and so on. Then input the number of BESSs to be installed.
*Step 2:* Generate the initial population by binary encoding using (2), (3) and (8).
*Step 3:* In the inner optimisation, OPF and BESS capacity adjustment are implemented to optimise the scheduling of BESS and adjust the capacity of BESS.

(1) OPF is adopted to optimise the charging/discharging power of BESS to achieve minimum network losses.
(2) On the basis of optimal scheduling of BESS, the step of BESS capacity adjustment is introduced. The BESS capacity optimised at a single node [17] can meet the requirements of one-day energy charging/discharging. When the capacity is larger, the DOD of each cycle will be reduced, leading to a longer battery lifetime. The trade-off between battery lifetime and investment cost of BESS has not been addressed in [17]. Incorporating the BESS lifetime prediction model, the BESS capacity adjustment proposed in this paper accounts for the impact of charging/discharging cycles and DODs on battery lifetime. Taking both capacity requirement and battery lifetime into considerations, this step

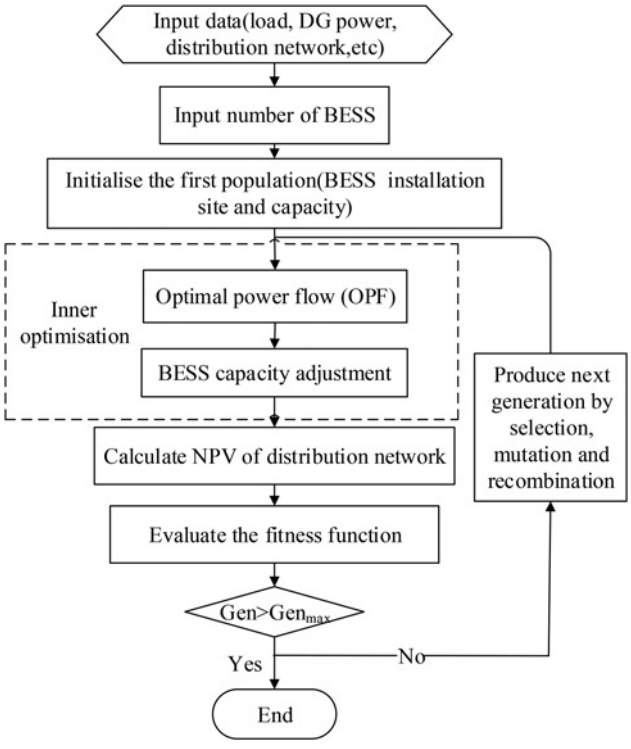


**Fig. 1** *Flowchart of optimal installation site and capacity*


*IET Gener. Transm. Distrib.*, 2016, Vol. 10, Iss. 3, pp. 601–607

implements capacity adjustment to further optimise the BESS capacity, which will lead to a lower total cost during the whole project life cycle.

*Step 4:* Calculate the NPV of BESS, the profits from line losses reduction and load shifting. By adding the three items together, the NPV of DN can be obtained.
*Step 5:* Calculate the fitness value of each individual in the population.

The next generation is produced by selection, mutation, and recombination. Steps 1–5 are repeated until the number of generation reaches its maximum. Finally, the optimisation process ends and the optimal solution is obtained.

The following section will introduce the modules of OPF, BESS capacity adjustment, and NPV calculation of DN.

### 3.2 Optimal power flow

The OPF model proposed by Carpinelli *et al.* [10] is adopted in this paper. Compared with the objectives of OPF in [10], reactive power and network upgrade are not considered in this work. When network losses minimisation is the only objective, BESS may be charged or discharged too much power at once. So the energy of BESS charging/discharging is added to the objective function. The input data are the installation locations of BESS and DG, and active/reactive power of DG. The control vector is charging/discharging power of BESS.

The objective function is expressed as

$$f = \max\left\{\alpha \Delta C_{\mathrm{LOSS}}(n) - \beta |E_{\mathrm{BESS}}(n)|\right\} \tag{11}$$

where $\Delta C_{\mathrm{LOSS}}(n)$ is the profit from network losses reduction at $n$th sampling period. $E_{\mathrm{BESS}}(n)$ is charging/discharging energy at $n$th sampling period. $\alpha$ and $\beta$ are weighting factors. The objective of this function is to maximise the profits from network losses reduction with minimum charging/discharging energy of BESS.

The constraints are presented as follows.

For charging

$$E_{\mathrm{BESS}}(n) = E_{\mathrm{BESS}}(n-1) + P_{\mathrm{BESS}}(n)\Delta t \cdot \eta_{\mathrm{C}} \tag{12}$$

For discharging

$$E_{\mathrm{BESS}}(n) = E_{\mathrm{BESS}}(n-1) - P_{\mathrm{BESS}}(n)\Delta t / \eta_{\mathrm{D}} \tag{13}$$

The constraint

$$E_{\mathrm{BESS(min)}} \le E_{\mathrm{BESS}}(n) \le E_{\mathrm{BESS(max)}} \tag{14}$$

where $E_{\mathrm{BESS}}(n-1)$ is BESS charging/discharging energy at time $n-1$. $E_{\mathrm{BESS(min)}}$, $E_{\mathrm{BESS(max)}}$ are the minimum and maximum energy limits of BESS, $P_{\mathrm{BESS}}(n)$ is BESS charging/discharging power at time $n$, and $\Delta t$ is the duration of charging/discharging.

Equations (12)–(16) show that BESS charging/discharging energy at sequence $n$ is determined by the energy at sequence $n-1$ and charging/discharging power at $n$. However, when energy in BESS is beyond the constraints, it is revised to equal to the minimum or maximum value.

The active power of BESS is constrained by the remaining energy at the previous time and the physical power limits of batteries.

For charging

$$P_{\mathrm{BESS}}(n) = \max\left\{P_{\mathrm{BESS\_}N}(n),\ \frac{P_{\max \mathrm{C}}}{\eta_{\mathrm{C}}},\ \frac{E_{\mathrm{BESS}}(n-1) - E_{\mathrm{BESS(max)}}}{\eta_{\mathrm{C}}\Delta t}\right\} \tag{15}$$

For discharging

$$P_{\mathrm{BESS}}(n) = \min\left\{P_{\mathrm{BESS\_}N}(n),\ P_{\max \mathrm{D}} \times \eta_{\mathrm{D}},\ \frac{\left[E_{\mathrm{BESS}}(n-1) - E_{\mathrm{BESS(min)}}\right]\eta_{\mathrm{D}}}{\Delta t}\right\} \tag{16}$$

where $P_{\mathrm{BESS}}(n)$ is BESS real charging/discharging power at sequence $n$, $P_{\mathrm{BESS\_N}}(n)$ is the required output power of BESS at time $n$. $P_{\mathrm{BESS\_N}}(n)$ is negative when charging, and positive when discharging. $P_{\mathrm{maxC}}$ and $P_{\mathrm{maxD}}$ are the maximum charging and discharging power limits.

Other equality constraints can be obtained from (4) and (5) and inequality constraints from (7), (9), and (10).

To guarantee that the SOC at the end of day is equal to the initial SOC, the sum of BESS charging/discharging energy needs to be zero during one day. Hence, some adjustments are made as follows. If the total discharged energy is less than the charged energy of BESS, the difference will be split to the peak load hours. This indicates that BESS needs to discharge more power at peak hours to keep the energy balance. In contrast, if the total discharged energy is larger than the charged energy, the difference will be split to off-peak load hours. The adjustments can help BESS gain more profit from load shifting.

### 3.3 BESS capacity adjustment

The power scheduling of BESS is determined by OPF at the previous step. The OPF is performed based on the BESS capacity at the initialisation of optimisation flow in Section 3.1. However, the required BESS capacity may be far less than the initialised BESS capacity, which cannot be fully utilised and decrease the economy efficiency. According to the physical characteristics of batteries, when the capacity is smaller, the DOD will be higher and the battery lifetime will decrease, and vice versa. Taking the impact of charging/discharging cycles and DOD on battery lifetime into account, the BESS capacity is optimised in this capacity adjustment step aiming at minimising the NPV of BESS in the whole project life cycle.

The battery life prediction model is introduced as follows.

*3.3.1 Battery lifetime prediction model:* Battery lifetime is a non-linear function of DOD. The rain-flow counting algorithm [18] is adopted to calculate the number of charging/discharging cycles and DOD for each cycle. The relationship between the number of cycles and DOD is described as

$$C_{\mathrm{F}} = a_1 + a_2\, \mathrm{e}^{a_3 \cdot \mathrm{DOD}} + a_4\, \mathrm{e}^{a_5 \cdot \mathrm{DOD}} \tag{17}$$

where $C_{\mathrm{F}}$ is the number of cycles to failure under a certain level of DOD, and $a_1$–$a_5$ are the constants fitted by Levenberg–Marquardt method based on the data provided by battery manufacturers.

The battery lifetime can be estimated according to the following equation

$$L_{\mathrm{BESS}} = \frac{1}{\sum C_{\mathrm{F}i}^{-1}} \frac{T_{\mathrm{sim}}}{T_{\mathrm{yr}}} \tag{18}$$

where $L_{\mathrm{BESS}}$ is the lifetime of BESS. $C_{\mathrm{F}i}$ is the number of cycles corresponding to the DOD of the $i$th cycle, $T_{\mathrm{sim}}$ is the simulation time period, $T_{\mathrm{yr}}$ represents 1 year, which means battery lifetime is measured in years. For example, if the battery discharges once a day with a constant DOD and the battery can withstand 1000 cycles for this DOD, the battery wears out 1/1000 per day, which is 365/1000 for one year. Then the battery lifetime is 1/(365/1000) year, which equals to 2.74 years.

*3.3.2 Capacity adjustment:* The flowchart of capacity adjustment is shown in Fig. 2.

The objective function is

$$f = \min\{\mathrm{NPV}_{\mathrm{BESS}}\} \tag{19}$$

$$\mathrm{NPV}_{\mathrm{BESS}} = \sum_{0}^{N_{\mathrm{P}}} \left[C_{\mathrm{BESS}}[i] \cdot (1 + F_{\mathrm{Dis}})^{-i}\right], \quad i = 0, 1, \ldots, N_{\mathrm{p}} \tag{20}$$

$$C_{\mathrm{BESS}}[i] = C_{\mathrm{Cap}}[i] + C_{\mathrm{Rep}}[i] + C_{\mathrm{Om}}[i] + C_{\mathrm{Sal}}[i] \tag{21}$$

The equality constraint is

$$P_{\mathrm{BESS}}(k)_{\mathrm{af}} = P_{\mathrm{BESS}}(k)_{\mathrm{be}} \tag{22}$$

where $\mathrm{NPV}_{\mathrm{BESS}}$ is the NPV of BESS. $N_{\mathrm{P}}$ is the number of planning years. $F_{\mathrm{Dis}}$ is the discount rate, and $C_{\mathrm{BESS}}[i]$ is the annual BESS cost of the $i$th year [18], $C_{\mathrm{Cap}}$ is the initial cost of BESS, $C_{\mathrm{Rep}}$ is the replacement cost. The number of replacements equals to $N_{\mathrm{p}}/L_{\mathrm{BESS}}$. $C_{\mathrm{Om}}$ is the operation and maintenance cost, and $C_{\mathrm{Sal}}$ is the salvage value. $P_{\mathrm{BESS}}(k)_{\mathrm{af}}$ and $P_{\mathrm{BESS}}(k)_{\mathrm{be}}$ are charging/discharging power of BESS after and before adjustment. This constraint ensures that the adjusted BESS capacity satisfies the required charging/discharging power.

GA is implemented to solve this optimisation model. First, BESS capacity is coded in binary code to generate the first population. Then BESS lifetime is estimated according to the battery lifetime prediction model. Further, the NPV of BESS can be calculated. At last, the fitness value of every individual in the population is calculated. The loop iterates until the number of generations reaches the maximum.

### 3.4 Economic evaluation model

BESS planning is usually a long-term problem. Hence, this paper uses NPV of DN as the optimisation objective. The formulations are expressed as follows

$$\mathrm{NPV}_{\mathrm{DN}} = \sum_{0}^{N_{\mathrm{P}}} \left[\mathrm{NCF}[i]*(1 + F_{\mathrm{Dis}})^{-i}\right], \quad i = 0, 1, \ldots, N_{\mathrm{p}} \tag{23}$$

$$\mathrm{NCF}[i] = C_{\mathrm{BESS}}[i] + C_{\mathrm{LOSS}}[i] + C_{\mathrm{LDS}}[i] \tag{24}$$

$$\Delta C_{\mathrm{LOSS}}[i] = \sum_{j}^{365} \sum_{k}^{24} \left[\Delta E_{\mathrm{LOSS}}[i, j, k]*M(k)\right] \tag{25}$$

$$C_{\mathrm{LDS}}[i] = \sum_{j}^{365} \sum_{k}^{24} \left[E_{\mathrm{BESS}}[i, j, k]*M(k)\right] \tag{26}$$

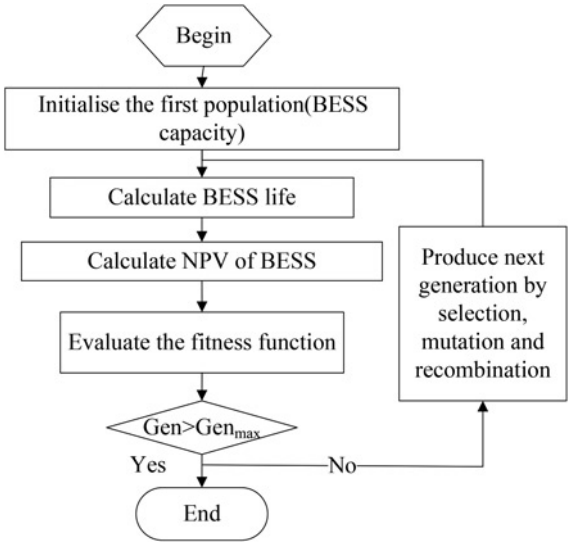


**Fig. 2** *Flowchart of capacity revision*

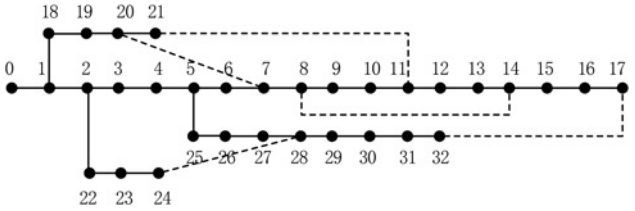


**Fig. 3** *DN of IEEE 33-bus system*

where $\mathrm{NPV}_{\mathrm{DN}}$ in (23) is the NPV of DN, NCF[$i$] is the total cost in the $i$th year, and $N_{\mathrm{p}}$ is the planning horizon, in years.

$C_{\mathrm{BESS}}$ in (24) is the total cost of BESS, which can be calculated by (19). $\Delta C_{\mathrm{LOSS}}$ is the profit from network losses reduction and $C_{\mathrm{LDS}}$ is the profit from load shifting.

$\Delta E_{\mathrm{LOSS}}[i, j, k]$ in (25) is the line loss at the $k$th hour of the $j$th day in the $i$th year. $M(k)$ is the electricity price at $k$th hour during one day.

$E_{\mathrm{BESS}}[i, j, k]$ in (26) is the charging/discharging energy at the $k$th hour of the $j$th day in the $i$th year.

## 4 Case study

### 4.1 Case data

In this section, the proposed method is implemented to the planning of BESS in a modified IEEE 33-bus system [19]. In this DN, the rated active load and reactive load is 3715 kW and 2300 kVar, respectively, and the base voltage is 12 kV. The basic system topology is depicted in Fig. 3. Two types of DGs, PV and WT, are installed in this modified system. The detailed installation site and rated power data of DG are shown in Table 1.

In this study, the time-of-use pricing mechanism is adopted. The electricity prices and time periods are: 0.1876 $/kWh from 9:00 to 21:00 (peak hours), 0.0608 $/kWh from 0:00 to 7:00 and 23:00 to 24:00 (off-peak hours), 0.1224 $/kWh from 7:00 to 9:00 and 21:00 to 23:00.

A lot of research has been carried out on the modelling of PV, WT and load. Such models in [20–22] are used in this paper. The output power of PV is generated based on the PV model in HOMER software [20], and Weibull distribution is used in the model of wind generation [21, 22], and Gaussian distribution is used in modelling load data [23]. Here, we provide time-series PV, WT, and load data that are generated by the above models.

The sampling period is 1 h. The daily power curves of load, wind power, and PV output are shown in Fig. 8 in Appendix. The active power of load and DGs are shown in Fig. 9. The out-of-limit hours, and maximum and minimum value (p.u.) of voltage without BESS for the 33 nodes can be found in Table 4. The upper and lower limits of voltage (p.u.) are 1.05 and 0.95, respectively.

Lithium battery is adopted in this planning study. The initial power and energy capacity of BESS are set to 100 kW and 100 kWh, respectively. The upper and lower limits of SOC are 100 and 40%, respectively. The branch flow limit is 8.92 MVA. According to industrial experience, the overall round-trip efficiency of the BESS is set to be 0.88. The discount rate is 2%.

**Table 1** Location and rated power of DG

| DG type | Installation site | Rated active power, kW | Rated reactive power, kVar |
|---|---|---|---|
| WT | 13 | 200 | 120 |
| WT | 15 | 100 | 60 |
| PV | 16 | 250 | 150 |
| WT | 17 | 200 | 120 |
| PV | 21 | 300 | 180 |
| PV | 24 | 200 | 120 |
| PV | 26 | 350 | 210 |
| WT | 30 | 200 | 120 |
| WT | 31 | 100 | 60 |


*IET Gener. Transm. Distrib.*, 2016, Vol. 10, Iss. 3, pp. 601–607

**Table 2** Economy of energy storage system

| BESS | $C_{Cap}$, \$/kWh | $C_{Rep}$, \$/kWh | $C_{Om}$, \$/kWh/year |
|---|---|---|---|
| lithium battery | 403 | 403 | 8 |

The project life cycle is 20 years. The economic parameters of the BESS are shown in Table 2.

The battery lifetime characteristic curve can be fitted based on the experimental data from battery manufacturers. The life characteristic curve of the lithium battery used in this study can be found in Fig. 10 in Appendix.

### 4.2 Optimisation results and comparison

The installation site and capacity of BESS are determined by the proposed method in this paper. In the GA, the length of chromosome is set to 20, and the maximum generation and size of population is set to 50. The variation probability is set to 0.03, and the crossover rate is set to 0.6. The optimal planning scheme is shown in Fig. 1.

To demonstrate the advantage of the proposed method, the optimisation results are compared with those obtained by the method in [10]. To ensure the fairness of comparison, both the proposed method and the method in [10] use the same case data in this testing system including load, DG, BESS, and electricity price, as well as the parameter settings in GA.

Table 3 shows the optimal results of the proposed method and the method in [10], including the optimal installation sites, energy and power capacity, lifetime, NPV of BESS, profit and the NPV of DN, when the numbers of BESSs are 1, 2, and 3, respectively. From Table 3, compared with the method in [10], the NPV of DN can be reduced by 29, 58, and 39%, respectively, when the numbers of BESS are 1, 2, and 3. The optimal installation sites obtained by the two methods are the same, and the profits from load shifting and network losses reduction are close. However, in the optimal scheme obtained by the proposed method, the BESS capacity is smaller and its cost is lower than that of the method in [10]. The reason is that the capacity of BESS from the initialisation may not be the best solution for the charging/discharging power obtained by OPF. In other words, the capacity may be larger than needed. In addition, the BESS capacity adjustment step in this paper further optimises the capacity considering the battery lifetime to lower the NPV of BESS. The lifetime is shorter but the capacity is smaller in the optimal scheme of the proposed method. It achieves an overall better economic performance, that is, lower NPV of BESS and NPV of DN.

### 4.3 BESS result

The charging/discharging power and SOC of BESS are shown in Figs. 4 and 5 when the number of BESS that needs to be allocated is 2.

The BESS at node 17 is charged with more power during 3:00–5:00 when the voltages at some nodes are higher than 1.05 as a result of light loads. Whereas the BESS at node 32 discharges more power during 12:00–16:00 when the voltages at some nodes are lower than 0.95 due to heavy loads. The maximum and minimum SOC are close to the preset upper and lower limits after the capacity adjustment, which indicates that the designed BESS capacity is the minimum that satisfies the load requirement. The results of BESS scheduling when the number of BESS is 1 and 3 are shown in Figs. 11–14, respectively, in Appendix. After the optimisation, none of the voltage is out of limit.

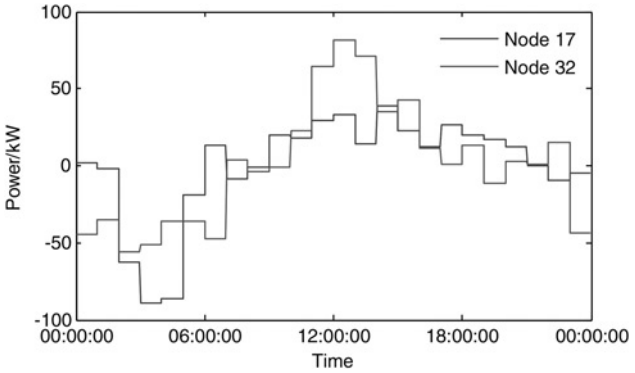


**Fig. 4** *Output power of two BESS (17th and 32th nodes)*

### 4.4 Relation between NPV of DN and number of BESS

With the increase of the number of BESSs, the variations of the NPV of DN are depicted in Fig. 6.

As shown in Fig. 6, the NPV of DN is the lowest when the number of BESSs to allocate is 2. Then the NPV is raised as the number of BESSs increases. From the results in Table 3, it can be observed that the NPV of DN with two BESSs is 48 and 32% lower than the NPVs of the cases with one BESS and three BESSs.

### 4.5 GA iterative process comparison

This paper introduces BESS capacity adjustment as one step in the inner optimisation, which can accelerate the process to find the optimal solution. The comparison between the optimisation process in this paper and in [10] is shown in Fig. 7.

Fig. 7 shows that the proposed method with capacity adjustment obtains the optimal solution with fewer generations. The method in [10] obtains the optimal solution after 40 generations, while this paper only takes 19 generations. In the proposed method, when the BESS capacity at initialisation cannot satisfy the constraints, the result in this generation will be abandoned, and the result before this generation will be saved. It can be concluded that the proposed method outperforms the method in [10] in terms of computational efficiency.

**Table 3** Optimal site, capacity, and economy of BESS

| Number of BESS | Optimation method | Optimal installation site | BESS energy capacity, kWh | BESS power capacity, kWh | BESS life, year | NPV of BESS, k\$ | Income from load shifting, k\$ | Income from line loss reduction, k\$ | NPV of DN, k\$ |
|---|---|---|---|---|---|---|---|---|---|
| 1 | this paper | 17 | 1332 | 231 | 6.87 | 1249.66 | −448.42 | −295.48 | 505.76 |
| | [10] | 17 | 1859 | 233 | 9.99 | 1347.36 | −384.57 | −247.09 | 715.84 |
| 2 | this paper | 17 | 450 | 80 | 8.03 | 380.48 | −336.33 | −264.92 | 262.65 |
| | | 32 | 585 | 81 | 8.29 | 483.39 | | | |
| | [10] | 17 | 775 | 169 | 7.9 | 662.49 | −381.45 | −228.96 | 622.43 |
| | | 32 | 726 | 110 | 8.9 | 570.34 | | | |
| 3 | this paper | 17 | 426 | 79 | 8.21 | 354.76 | −312.57 | −271.09 | 385.16 |
| | | 32 | 379 | 54 | 8.15 | 316.98 | | | |
| | | 31 | 277 | 43 | 5.76 | 297.09 | | | |
| | [10] | 17 | 522 | 89 | 9.63 | 388.57 | −332.24 | −270.43 | 631.11 |
| | | 32 | 513 | 76 | 7.22 | 465.84 | | | |
| | | 31 | 435 | 83 | 7.67 | 379.39 | | | |

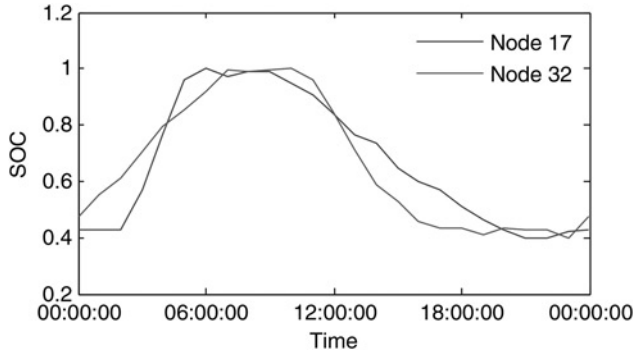


**Fig. 5** *SOC of two BESS (17th and 32th nodes)*

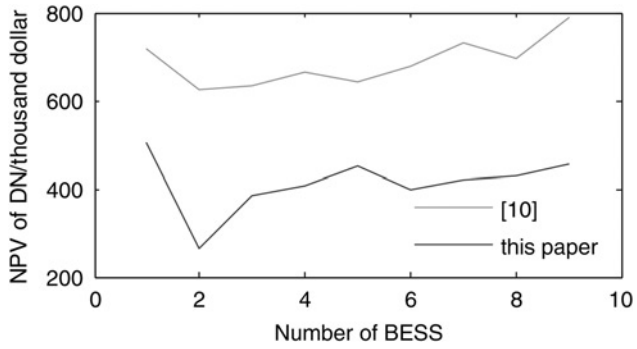


**Fig. 6** *Variations of NPV of DN along with the number of BESS*

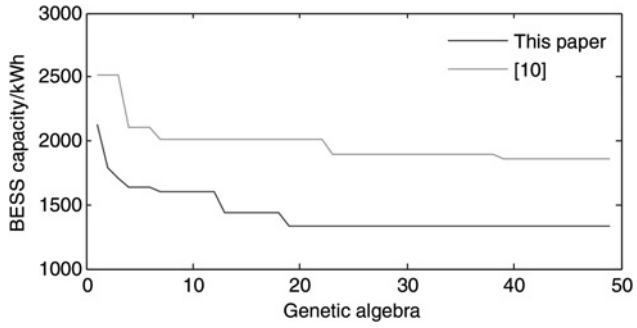


**Fig. 7** *Comparison between the optimisation process in this paper and [10]*

## 5 Conclusions

A novel bi-level optimisation model is proposed to determine the optimal installation site and capacity of BESS in DN. In the inner optimisation, to account for the impact of charging/discharging cycles and DODs on battery lifetime, the BESS capacity adjustment step is introduced to lower the NPV of DN and accelerate the convergence speed of GA. The proposed method can be applied to multiple BESS planning in DN. The simulation results on a modified IEEE 33-bus demonstrate the effectiveness of the proposed method and a comparative study shows its superiority over the method in [10]. The contributions of the paper are summarised as follows.

(i) A bi-level optimisation model is built to optimise installation site and capacity of BESS with the objective of minimising the NPV of DN in the project life cycle.

(ii) In the inner loop optimisation, the method of capacity adjustment is proposed to minimise the cost of BESS. The battery lifetime prediction model is incorporated into the optimisation model for BESS capacity adjustment. With the capacity adjustment, the optimal scheme can achieve a smaller BESS capacity and lower NPV of DN while satisfying system requirements.

(iii) The proposed solution method converges faster than the existing method in [10]. The results of the comparative study show that the proposed method can reduce the number of generations in GA for searching the optimum.

## 6 Acknowledgments

This paper is funded in National High Technology Research and Development of China (863 program) (2011AA05A117) and Project Supported by the National Natural Science Foundation of China (51477112).

## 7 References

1 Li, Q., Choi, S.S., Yuan, Y., *et al.*: 'On the determination of battery energy storage capacity and short-term power dispatch of a wind farm', *IEEE Trans. Sustain. Energy*, 2011, **2**, (2), pp. 148–158
2 Hashemi, S., Ostergaard, J., Yang, G.: 'A scenario-based approach for energy storage capacity determination in LV grids with high PV penetration', *IEEE Trans. Smart Grid*, 2014, **5**, (3), pp. 1514–1522
3 Makarov, Y.V., Du, P., Kintner-Meyer, M.C., *et al.*: 'Sizing energy storage to accommodate high penetration of variable energy resources', *IEEE Trans. Sustain. Energy*, 2012, **3**, (1), pp. 34–40
4 Abbey, C., Joos, G.: 'A stochastic optimization approach to rating of energy storage systems in wind-diesel isolated grids', *IEEE Trans. Power Syst.*, 2009, **24**, (1), pp. 418–426
5 Zheng, Y., Dong, Z.Y., Luo, F.J., *et al.*: 'Optimal allocation of energy storage system for risk mitigation of discos with high renewable penetrations', *IEEE Trans. Power Syst.*, 2014, **29**, (1), pp. 212–220
6 Karanki, S.B., Xu, D., Venkatesh, B., *et al.*: 'Optimal location of battery energy storage systems in power distribution network for integrating renewable energy sources'. Energy Conversion Congress and Exposition (ECCE), 2013, pp. 4553–4558
7 Nick, M., Cherkaoui, R., Paolone, M.: 'Optimal allocation of dispersed energy storage systems in active distribution networks for energy balance and grid support', *IEEE Trans. Power Syst.*, 2014, **29**, (5), pp. 2300–2310
8 Hung, D.Q., Mithulananthan, N.: 'Community energy storage and capacitor allocation in distribution systems'. Proc. of 2011 Australasian Universities Power Engineering Conf. (AUPEC), 2011
9 Carpinelli, G., Mottola, F., Proto, D., *et al.*: 'Optimal allocation of dispersed generators, capacitors and distributed energy storage systems in distribution networks'. Proc. of IEEE Int. Symp. on Modern Electric Power Systems (MEPS'10), 2010
10 Carpinelli, G., Mocci, S., Mottola, F., *et al.*: 'Optimal integration of distributed energy storage devices in smart grids', *IEEE Trans. Smart Grid*, 2013, **4**, (2), pp. 985–995
11 Celli, G., Mocci, S., Pilo, F., *et al.*: 'Optimal integration of energy storage in distribution networks'. 2009 IEEE Bucharest PowerTech, 2009
12 Ghofrani, M., Arabali, A., Etezadi-Amoli, M., *et al.*: 'A framework for optimal placement of energy storage units within a power system with high wind penetration', *IEEE Trans. Sustain. Energy*, 2013, **4**, (2), pp. 434–442
13 Law, M.A.: 'Using net present value as a decision–making tool', *Air Med. J.*, 2004, **23**, pp. 28–33
14 Chacra, F.A., Bastard, P., Fleury, G., *et al.*: 'Impact of energy storage costs on economical performance in a distribution substation', *IEEE Trans. Power Syst.*, 2005, **20**, (2), pp. 684–691
15 Chen, C., Duan, S., Cai, T., *et al.*: ' Optimal allocation and economic analysis of energy storage system in microgrids', *IEEE Trans. Power Electron.*, 2011, **26**, (10), pp. 2762–2773
16 Gaun, A., Rechberger, G., Renner, H.: 'Probabilistic reliability optimization using hybrid genetic algorithms'. Electric Power Quality and Supply Reliability Conf. (PQ), 2010, pp. 151–158
17 Xiao, J., Bai, L., Li, F., *et al.*: 'Sizing of energy storage and diesel generators in an isolated microgrid using discrete Fourier transform (DFT)', *IEEE Trans. Sustain. Energy*, 2014, **5**, (3), pp. 907–916
18 Manwell, J., Rogers, A., Hayman, G., *et al.*: 'Hybrid2: a hybrid system simulation model theory manual' (Renewable Energy Research Laboratory, Department of Mechanical Engineering, University of Massachusetts, 2006)
19 Goswami, S.K., Basu, S.K.: 'A new algorithm for the reconfiguration of distribution feeders for loss minimization', *IEEE Trans. Power Deliv.*, 1992, **7**, (3), pp. 1484–1491
20 Xiao, J., Bai, L., Wang, C., *et al.*: 'Method and software for planning and designing of microgrid'. Zhongguo Dianji Gongcheng Xuebao (Proc. of the Chinese Society of Electrical Engineering), 2012, vol. 32, no. 25
21 Hetzer, J., Yu, D.C., Bhattarai, K.: 'An economic dispatch model incorporating wind power', *IEEE Trans. Energy Convers.*, 2008, **23**, (2), pp. 603–611
22 Xiao, J., Bai, L., Lu, Z., *et al.*: 'Method, implementation and application of energy storage system designing', *Int. Trans. Electr. Energy Syst.*, 2014, **24**, (3), pp. 378–394
23 Zou, K., Agalgaonkar, A.P., Muttaqi, K.M., *et al.*: 'Distribution system planning with incorporating DG reactive capability and system uncertainties', *IEEE Trans. Sustain. Energy*, 2012, **3**, (1), pp. 112–123

## 8 Appendix

See Figs. 8–14 and Table 4.

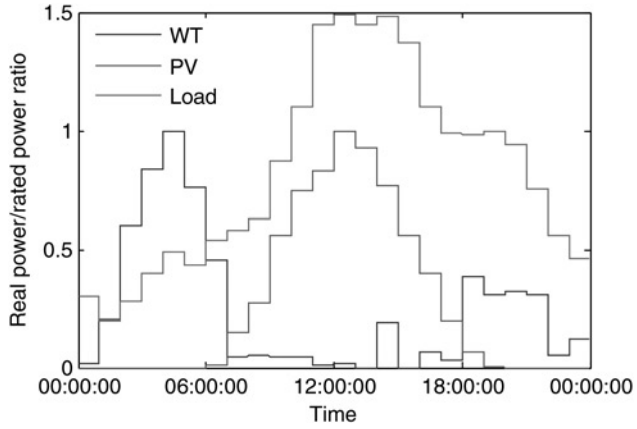


**Fig. 8** *Load and DG real power/rated power ratio*

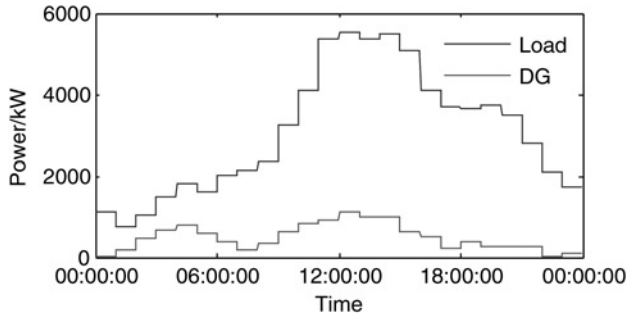


**Fig. 9** *Load and DG real power in DN*

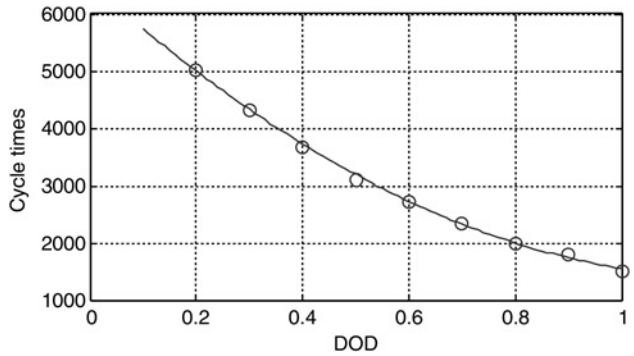


**Fig. 10** *Battery life cycle characteristics*

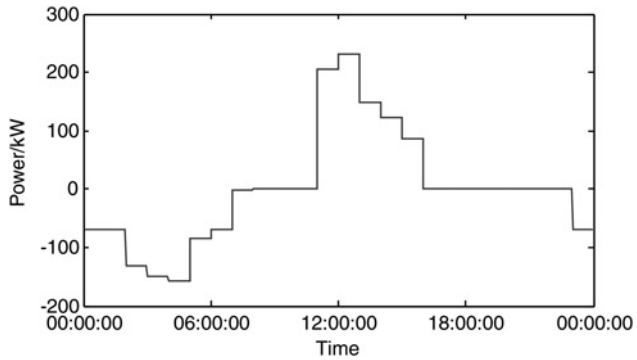


**Fig. 11** *Power of one battery (17th node)*

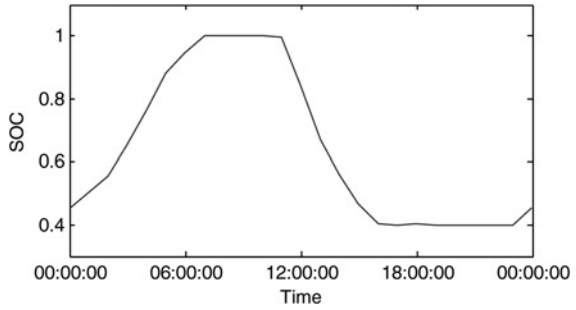


**Fig. 12** *SOC of one battery (17th node)*

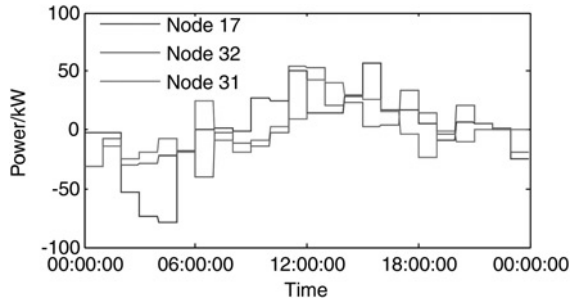


**Fig. 13** *Power of three batteries (17th, 32th, and 31th nodes)*

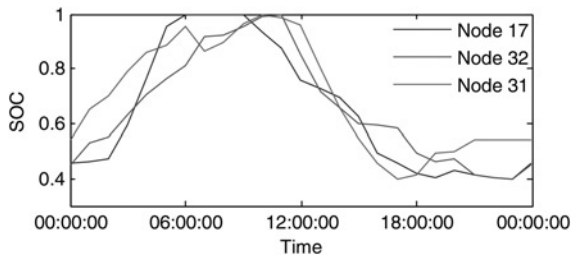


**Fig. 14** *SOC of three batteries (17th, 32th, and 31th nodes)*

**Table 4** 24 h voltage state of 33 buses without BESS

| Node | Hours out of limit | Minimum value p.u. | Maximum value p.u. |
|---|---|---|---|
| 1 | 0 | 1.050 | 1.05 |
| 2 | 0 | 1.046 | 1.049 |
| 3 | 0 | 1.027 | 1.048 |
| 4 | 0 | 1.018 | 1.047 |
| 5 | 0 | 1.008 | 1.047 |
| 6 | 0 | 0.984 | 1.046 |
| 7 | 0 | 0.979 | 1.046 |
| 8 | 0 | 0.973 | 1.046 |
| 9 | 0 | 0.966 | 1.047 |
| 10 | 0 | 0.959 | 1.049 |
| 11 | 0 | 0.958 | 1.049 |
| 12 | 0 | 0.956 | 1.049 |
| 13 | 4 | 0.949 | 1.052 |
| 14 | 5 | 0.947 | 1.054 |
| 15 | 6 | 0.946 | 1.055 |
| 16 | 7 | 0.945 | 1.056 |
| 17 | 6 | 0.944 | 1.058 |
| 18 | 8 | 0.943 | 1.059 |
| 19 | 0 | 1.046 | 1.049 |
| 20 | 0 | 1.043 | 1.049 |
| 21 | 0 | 1.042 | 1.049 |
| 22 | 0 | 1.041 | 1.048 |
| 23 | 0 | 1.022 | 1.047 |
| 24 | 0 | 1.013 | 1.045 |
| 25 | 0 | 1.010 | 1.045 |
| 26 | 0 | 0.981 | 1.045 |
| 27 | 0 | 0.978 | 1.045 |
| 28 | 0 | 0.960 | 1.044 |
| 29 | 5 | 0.947 | 1.043 |
| 30 | 5 | 0.941 | 1.043 |
| 31 | 5 | 0.935 | 1.044 |
| 32 | 5 | 0.933 | 1.044 |
| 33 | 5 | 0.933 | 1.043 |